Transverse Instability of Optical Spatiotemporal Solitons in Quadratic Media

Xiang Liu, Kale Beckwitt, and Frank Wise
Department of Applied Physics, Cornell University, Ithaca, New York 14853
(Received 10 April 2000)

We present experimental and numerical observations of transverse instability in quadratic media under conditions that emphasize the inherently spatiotemporal and multidimensional nature of the wave propagation. Intensity-dependent beam filamentation is shown to be closely connected to the periodic evolution of quadratic solitons, and implications for the generation of three-dimensional spatiotemporal solitons are discussed.

PACS numbers: 42.65.Tg, 05.45.Yv, 42.65.Sf

Optical solitons are localized electromagnetic waves that propagate in nonlinear media with dispersion and/or diffraction. Extensive theoretical and experimental understanding of both spatial and temporal optical solitons has been accumulated [1]. Much less is known experimentally about spatiotemporal solitons (STS), which result from the simultaneous balance of diffraction and dispersion by self-focusing and nonlinear phase modulation, respectively. To date, STS have been generated only in quadratic media [2,3]; pulses overcome diffraction in one transverse spatial dimension as well as group-velocity dispersion (GVD) to reach stable or periodically stable beam size and pulse duration, and diffraction occurs in the remaining transverse spatial dimension. One of the major goals in the field of soliton physics is the production of pulses of light that are localized in all dimensions, which we will refer to as three-dimensional (3D) STS [4]. In addition to the scientific interest in the generation of 3D STS, such pulses could be the basis of ultrafast optical digital logic in the future [5].

The stability of solitons is a crucial issue, and more generally the instabilities of waves propagating in nonlinear systems have been the subject of much study, since they can lead to dramatic physical effects. One particular type of instability is that which occurs when a soliton propagates in a medium of higher dimensionality than its own. Such an instability is referred to as a transverse instability (TI) or a modulation instability (MI) [6], and may lead to a beam breaking into a number of fragments. The fragments may in turn form solitons in subsequent evolution. These processes have been studied theoretically for cubic [7–10] and quadratic [11–16] nonlinear media.

Instabilities of this type are observed in the evolution of optical beams in several classes of materials. For example, bright soliton stripes in a bulk photorefractive medium were found to break up into a sequence of two-dimensional (2D) self-trapped beams [17]. In addition, pairs of vortex solitons can be generated by the TI of dark soliton stripes [18]. The decay of ring-shaped beams into higher-dimensional solitons has been observed in Rb vapor [19], in a quadratic nonlinear crystal [20], and in photorefractive media [21]. Perhaps most pertinent to the work described in this Letter is the experimental observation of filamentation of stationary spatial solitons in quadratic nonlinear media [22].

It is difficult to create an experimental environment that supports 3D STS, so it is intriguing that instabilities of lower-dimensional solitons offer a potential route to formation of 3D STS. In numerical studies, Akhmediev and co-workers found that a stationary 2D solitary stripe propagating in a medium with anomalous GVD and a saturable nonlinearity breaks up into 3D STS [9]. A similar investigation of quadratic media concludes that 2D spatial solitons decay into a train of quasistable 3D solitons owing to MI [23]. Baboiu and Stegeman [16] analyzed the effects of spatial modulation imposed on a one-dimensional (1D) spatial soliton (a beam in the form of a stripe) in a quadratic medium. The initial state of the process we address here is already a temporal soliton, or a pulse evolving to a temporal soliton. Thus, a similar instability of 2D spatiotemporal solitons could be expected to produce a structure localized in the remaining transverse dimension, i.e., a 3D STS.

Here we describe observations of the TI of STS. 2D STS in the form of a spatial stripe are generated under conditions (namely, space-time anisotropy) that highlight the essential spatiotemporal nature of the STS. Calculations agree with the experimental results and demonstrate that the TI is directly influenced by the periodic evolution of quadratic STS.

The diffraction, dispersion, and nonlinear lengths characterizing pulse propagation in a quadratic medium are $L_{DFx(y)} = k\omega_{0x(y)}^2/2$, $L_{DS} = 0.322\tau_0^2/|\beta^{(2)}|$, and L_{NL} (the length over which the accumulated nonlinear phase shift is 1), respectively, where λ is the fundamental-harmonic (FH) wavelength, $\omega_{0x(y)}$ is the $x(y)$-dimension beam waist, and $\beta^{(2)}$ is the GVD. The characteristic length over which the FH and second-harmonic (SH) pulses move away from each other in time is $L_{\mathrm{GVM}} = c\tau_0/(n_{1g} - n_{2g})$ where n_{1g} and n_{2g} are the group indices at the FH and SH frequencies, respectively, and τ_0 is the full width at half maximum pulse duration.

In the absence of group-velocity mismatch (GVM), time is formally equivalent to the transverse space dimensions, and one might expect the instability of 2D STS to be

fundamentally the same as the instability of 2D spatial solitons. However, we will describe experiments performed in the presence of large GVM: $L_{DS}/L_{\mathrm{GVM}} = 3$. In linear propagation the FH and SH pulses would move away from each other by 3 times the pulse duration in one characteristic length. In addition, the ratio of the FH to SH dispersion lengths does not equal the ratio of the diffraction lengths ($L_{DS1}/L_{DS2} \neq L_{DF1}/L_{DF2}$). Therefore, the problem is highly anisotropic in the transverse dimensions, and the spatiotemporal nature is essential.

To generate STS, we match L_{DS} and L_{NL} to L_{DF}. A diffraction grating introduces large and anomalous GVD [24] and in turn allows convenient characteristic lengths of $\sim$5 mm. Pulses of duration 120 fs and energy up to 1 mJ at a wavelength of 800 nm are produced by a Ti:sapphire regenerative amplifier. The beam is compressed in one transverse direction to $\sim$60 μm, producing a spatial stripe with aspect ratio 30:1. Experiments were performed with 17- and 25-mm long barium metaborate (BBO) crystals cut for type-I phase-matching. These lengths allow for propagation over 3.5 and 5.5 characteristic lengths at the FH frequency, and propagation through the two adjoined crystals corresponds to 9 characteristic lengths. BBO conveniently provides an environment with large GVM, and has negligible two-photon absorption at the wavelengths of interest. These properties led us to choose BBO over $LiIO_3$, which was used in previous experiments on STS [2]. Details of the experimental setup are described in Ref. [3].

Stable 2D STS (Fig. 1) are generated for $I_0 \approx 9$ GW/cm^2 and $\Delta k \approx -24\pi$ cm^{-1} [3]. These are referred to as "walking" solitons because their velocity depends on their FH/SH energy distribution [25–27]. With fixed phase mismatch, increasing the intensity to $I_0 \approx 11$ GW/cm^2 causes the STS to break up along the unconfined transverse dimension. At $z = 3.5L_{DF}$ the beam breaks into a set of elliptically shaped filaments with minor axis $\sim$65 μm and average aspect ratio $\sim$4:3. After propagation to $z = 5.5L_{DF}$ the filaments become nearly circular (Fig. 1) with diameter $\sim$65 μm (close to the confined dimension of the 2D STS). A similar

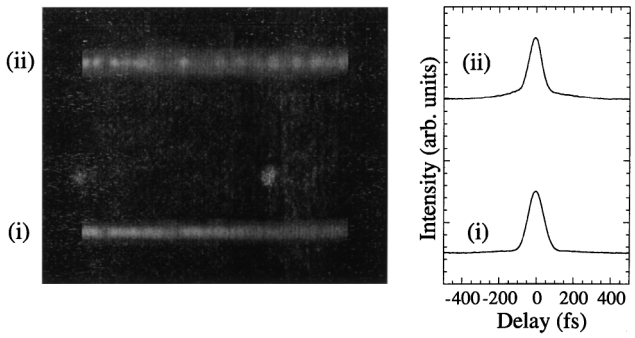

FIG. 1. Beam waist (left) and temporal profile (right) at $z = 5.5L_{DF}$ (25 mm) for (i) 2D STS formation at $I_0 \approx 9$ GW/cm^2 and (ii) typical filamentation near $I_0 \approx 11$ GW/cm^2. For both $\Delta k \approx -24\pi$ cm^{-1}.

filamentation of the 2D STS is observed when the phase mismatch is reduced in magnitude with fixed I_0, an alternate way to increase the nonlinear phase shift. Lower-contrast photographs indicate that a weak ($\sim$25% of the total power) uniform background of dispersive FH and SH light accompanies the filamentation of the beam.

We also monitored the pulse temporal profile as the intensity was varied. The intensity autocorrelations of the STS and a single filament are shown in Fig. 1. The pulse duration decreases slightly with I_0 and reaches a minimum for values $\sim$10% above the threshold for filamentation. Higher intensities then increase the apparent pulse duration. This will be discussed below.

To confirm that TI can cause the observed breakup of STS, we solved the coupled wave equations in the presence of noise. The parameters chosen for the numerical simulations are similar to those of the experiments, except that the aspect ratio of the beam is limited to $\sim$10:1 by our computing capability. When Gaussian intensity fluctuations of random spatial frequency and magnitude are imposed on the input beam, clear filamentation is observed. Figure 2 shows the beam profile at different incident intensities, as in Fig. 1. Figure 3 shows the spatiotemporal profiles of the FH and SH waves in the x-t plane at $y = 0$ and $z = 3.5L_{DF}$, right after filamentation occurs. The mutually trapped FH and SH waves comprising each filament

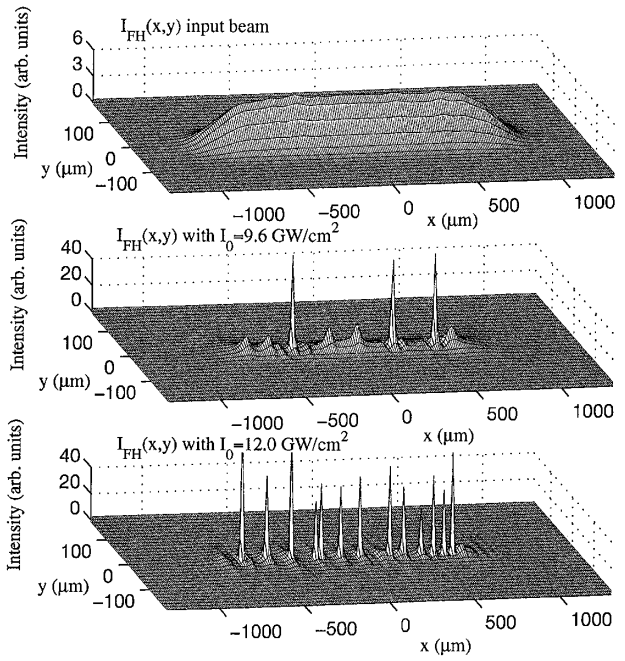

FIG. 2. Numerical simulation of pulse evolution in the presence of noise (along x). Time integrated spatial profiles of the input beam (top) and the beam profiles at $z = 2.7L_{DF}$ (12 mm), with $I_0 = 9.6$ GW/cm^2 (middle) and $I_0 = 12.0$ GW/cm^2 (bottom). In all cases, $\Delta k = -24\pi$ cm^{-1}. The STS formed with I_0 below the threshold for filamentation are similar to the input beam but with slight focusing in x and no noise.

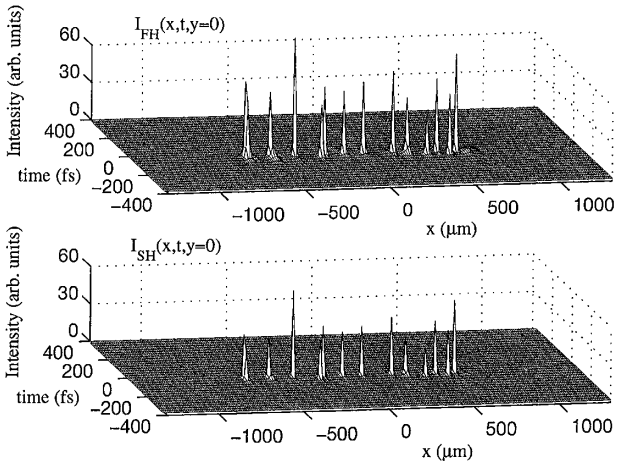

FIG. 3. Numerical simulation of generated FH (upper) and SH (lower) filaments after $2.7L_{DF}$ (12 mm) propagation with $I_0 = 12$ GW/cm^2 and $\Delta k = -24\pi$ cm^{-1}. Notice the mutual trapping of the FH and SH filaments in the time domain and the walking soliton behavior of the filaments.

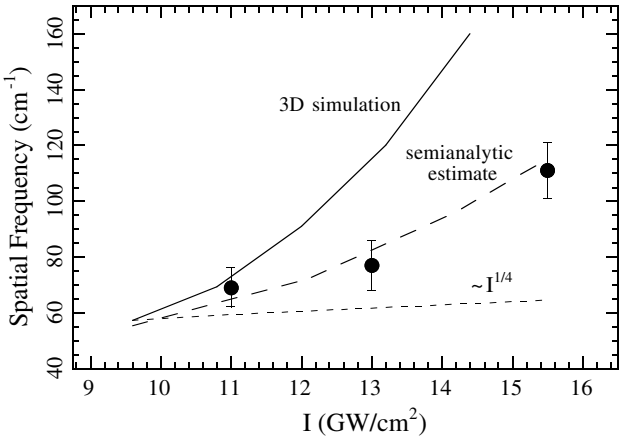

FIG. 4. Dependence of filament spatial frequency on incident intensity. The circles represent experimental data and the solid line shows 3D simulation results. The short-dashed line indicates $I^{1/4}$ growth from the low intensity data point and the long dashed line represents semianalytic calculation of the spatial frequency from peak intensity data based on 2D simulation results. Experimental spatial frequencies were obtained by Fourier transformation of cuts through data, as in Fig. 1.

propagate together in time and space, forming a 3D STS. Because they evolve from fluctuations, each filament has different FH/SH energy content and thus different velocity (Fig. 3). At higher I_0 the filamentation occurs earlier, so there is more time for the filament pulses to propagate with distinct velocities. Under experimental conditions corresponding to the simulations of Fig. 3, the apparent pulse duration measured with the entire beam is about twice that of the STS, in good agreement with the variation of temporal positions of the filament pulses.

One of the signatures of TI is the dependence of the spatial filament frequency on incident intensity (Fig. 4). Remarkably, the frequency increases superlinearly with I_0. The superlinear behavior can be understood as a direct consequence of the periodic evolution of STS. As a simplified model of the quadratic medium in the limit of large phase mismatch, consider the spatial nonlinear Schrödinger equation. The maximum TI gain occurs at frequency $\Omega_{\max} \approx (1/2\pi)\,(0.14\lambda L_{DF})^{-1/2} \sim (\Delta\Phi_{NL})^{1/2}$, where the latter relation follows from $L_{DF} = L_{NL}$. In Kerr media, $\Omega_{\max} \sim I^{1/2}$, while in quadratic media under conditions of saturation, $\Omega_{\max} \sim I^{1/4}$ [22]. Filamentation due to TI is most likely to occur at positions of highest intensity, and the maximum intensity of STS varies rapidly with the input intensity [3]. As an example, with I_0 only 40% larger than the threshold for STS formation, $I \sim 9I_0$ is reached twice per soliton period [3]. Evaluation of the expression for $\Omega_{\max}$ above using the peak intensities obtained from numerical simulations produces the semianalytic estimate in Fig. 4. The superlinear dependence is reproduced, although the quantitative agreement with experiment should not be taken seriously. 3D numerical solutions predict an even stronger dependence on input intensity. We attribute most of the discrepancy between simulation and experiment to the neglect of a small nonlinear loss at the SH frequency in the simulations. Furthermore, the simulations do suggest that some self-focusing in the unconfined direction (Fig. 2) contributes to the increased intensity, and, in turn, spatial frequency. The increased dimensionality enhances the intensity dependence as a result of increased intensity oscillation during soliton propagation, in contrast to MI observed previously with continuous waves (leading to temporal solitons) [28] and with 1D spatial solitons (leading to 2D spatial solitons) [22].

For $I_0 \approx 16$ GW/cm^2 (about 1.5 times the intensity at which the beam first breaks up), the filaments begin to distort and exhibit spatial frequency chirp, the manifestations of strong self-focusing and incipient collapse arising from $\chi^{(3)}$. We believe that filamentation of a periodic STS occurs at powers high enough for Kerr self-focusing to become significant; this is observed in numerical simulations. At large-enough phase mismatch and/or high-enough intensity, collapse of the 2D STS occurs before filamentation.

It is interesting to consider the nature of the experimental filaments themselves. The use of angular dispersion to create GVD in the present experiment eventually precludes the formation of 3D STS. This angular dispersion will broaden the beam in the unfocused direction by $\sim$100 μm/cm, which becomes appreciable for the filaments. The filaments reach minimum spatial and temporal dimensions at $z \sim 5.5L_{DF}$, at which point they are destabilized by the spatial broadening from angular dispersion. After traversing an additional 3.5 characteristic lengths, the beam (pulse) broadens to $\sim$125 μm ($\sim$280 fs). The angular dispersion broadens the filaments after formation, but does not affect the breakup dynamics and observed spatial filament frequencies.

In conclusion, we have observed a TI of 2D STS in quadratic media. The TI is intimately connected to the periodic nature of quadratic STS. An exciting implication of this work is that this process should provide one means of producing 3D STS. As emphasized originally by Kanashov and Rubenchik [12], only the 3D STS is truly stable; all lower-dimensional solitons are susceptible to TI. Thus, the TI of the 2D bound state offers a route to the "self-assembly" of 3D STS if the required GVD is produced without angular dispersion.

This work was supported by the National Science Foundation under Award No. ECS-9612255, the National Institutes of Health under Award No. RR10075, and the Cornell Theory Center. The authors thank Y. Kivshar, D. Skryabin, B. Malomed, and P. Di Trapani for valuable discussions.

[1] Special issue of J. Opt. Soc. Am. B **14**, 2950–3253 (1997); special issue of Opt. Quantum Electron. **30**, 501–937 (1998).
[2] X. Liu, L. J. Qian, and F. W. Wise, Phys. Rev. Lett. **82**, 4631 (1999).
[3] X. Liu, K. Beckwitt, and F. Wise, Phys. Rev. E **62**, 1328 (2000).
[4] Y. Silberberg, Opt. Lett. **15**, 1282 (1990).
[5] R. Macleod, K. Wagner, and S. Blair, Phys. Rev. A **52**, 3254 (1995).
[6] Y. S. Kivshar and D. E. Pelinovsky, Phys. Rep. **331**, 117 (2000).
[7] V. E. Zakharov and A. M. Rubenchik, Sov. Phys. JETP **38**, 494 (1974).
[8] G. S. McDonald, K. S. Syed, and W. J. Firth, Opt. Commun. **95**, 281 (1993).
[9] N. N. Akhmediev, V. I. Korneev, and R. F. Nabiev, Opt. Lett. **17**, 393 (1992); N. N. Akhmediev and J. M. Soto-Crespo, Phys. Rev. A **47**, 1358 (1993).
[10] B. J. Eggleton, C. Martijn de Sterke, A. B. Aceves, J. E. Sipe, T. A. Strasser, and R. E. Slusher, Opt. Commun. **149**, 267 (1998).
[11] Z. H. Musslimani and B. A. Malomed, Physica (Amsterdam) **123D**, 235 (1998).
[12] A. A. Kanashov and A. M. Rubenchik, Physica (Amsterdam) **4D**, 122 (1981).
[13] S. Trillo and P. Ferro, Opt. Lett. **20**, 438 (1995).
[14] H. He, P. D Drummond, and B. A. Malomed, Opt. Commun. **54**, 896 (1996).
[15] A. De Rossi, S. Trillo, A. V. Buryak, and Y. S. Kivshar, Opt. Lett. **22**, 868 (1997).
[16] D.-M. Baboiu and G. I. Stegeman, Opt. Quantum Electron. **30**, 937 (1998).
[17] A. V. Mamaev, M. Saffman, and A. A. Zozulya, Europhys. Lett. **35**, 25 (1996).
[18] A. V. Mamaev, M. Saffman, and A. A. Zozulya, Phys. Rev. Lett. **76**, 2262 (1996); V. Tikhonenko, J. Christou, B. Luther-Davies, and Y. S. Kivshar, Opt. Lett. **21**, 1129 (1996).
[19] V. Tikhonenko, J. Christou, and B. Luther-Davies, J. Opt. Soc. Am. B **12**, 2046 (1995).
[20] D. V. Petrov, L. Torner, J. Martorell, R. Vilaseca, J. P. Torres, and C. Cojocaru, Opt. Lett. **23**, 1444 (1998).
[21] Z. Chen, M.-F. Shih, M. Segev, D. W. Wilson, R. E. Muller, and P. D. Maker, Opt. Lett. **22**, 1751 (1997).
[22] R. A. Fuerst, D. M. Baboiu, B. Lawrence, W. E. Torruellas, G. I. Stegeman, S. Trillo, and S. Wabnitz, Phys. Rev. Lett. **78**, 2756 (1997).
[23] D. V. Skryabin and W. J. Firth, Opt. Commun. **148**, 79 (1998).
[24] O. E. Martinez, IEEE J. Quantum Electron. **25**, 2464 (1989).
[25] L. Torner, D. Mazilu, and D. Mihalache, Phys. Rev. Lett. **77**, 2455 (1996).
[26] D. Mihalache, D. Mazilu, L.-C. Crasovan, and L. Torner, Opt. Commun. **137**, 113 (1997).
[27] C. Etrich, U. Peschel, F. Lederer, and B. A. Malomed, Phys. Rev. E **55**, 6155 (1997).
[28] K. Tai, A. Hasegawa, and A. Tomita, Phys. Rev. Lett. **56**, 135 (1986).